Mine Water Environ (2017) 36:104–113
DOI 10.1007/s10230-016-0414-4

TECHNICAL ARTICLE

Effects of Coal Mining on Shallow Water Resources in Semiarid Regions: A Case Study in the Shennan Mining Area, Shaanxi, China

Wei Qiao[1,2] · Wenping Li[1] · Tao Li[3] · Jinyuan Chang[4] · Qiqing Wang[1]

Received: 27 January 2015 / Accepted: 16 August 2016 / Published online: 22 September 2016

Abstract The Shennan mining area in northern Shanxi Province is located in a semiarid area where surface and near-surface water resources are very valuable. Mining-induced fractures can cause these shallow water resources to leak. The overburden strata were divided into engineering geology rock groups and a comparative analysis was calculated based on the height of the water-conducting fractured zone and the key stratum theory, using both an empirical formula and a fitting formula. The influence of coal mining on the shallow water resources was divided into four types: serious, moderate, slight, and no water loss. Finally, a water resource leakage differentiation graph was produced for the study area. The results can be used to guide coal extraction in the study area and to protect the area's shallow water resources.

Keywords Water protection · Key strata · Water-conducting fractured zone · Pumping test · Water equilibrium

✉ Wei Qiao
qiaowei@cumt.edu.cn

1 Colliery Engineering Geological Research Institute, School of Resources and Earth Science, China University of Mining and Technology, No. 1, Daxue Rd, Xuzhou 221116, Jiangsu, People's Republic of China

2 Postdoctoral Workstation, Yankuang Group, Zoucheng 273500, Shandong, People's Republic of China

3 Shaanxi Coal and Chemical Industry Group Ltd, Xi'an 710065, Shaanxi, People's Republic of China

4 University of Shaoxing, Shaoxing 312000, Zhejiang, People's Republic of China

Introduction

Eleven of China's 14 large coal-producing regions are located in arid and semi-arid areas (Qiao et al. 2014; Sun et al. 2012). Water protection is a major issue for large underground mines in such areas, especially in the Shaanxi, Inner Mongolia, and Xinjiang provinces in northwest China. The effect of coal mining on water resources has been widely studied (Adam and Paul 2000; Andreas and Nikola 2011; Karen and Paul 2006; Tan 2008; Wu and Chen 2008; Wu and Li 2002; Zhang et al. 2009) and measures to protect alluvial aquifers in arid and semiarid mining areas were established several decades ago (Thomas and Anderson 1976; Hickcox 1980). Researchers have defined zones using various parameters to describe the order of fracture severity and groundwater effects from the immediate roof towards the surface (Kendorski 1993; Peng 2008; Singh and Atkins 1982; Tieman and Rauch 1987). China has developed some coal mining practices and experimental techniques to protect aquifers and surface water resources and reduce the threat of water inrush (Liu 1981).

Longwall mining, which revolutionised underground coal mining with its capacity for safe, cost effective, and efficient large-scale extraction, has been extensively used around the world. The overburden can be disturbed from the seam level all the way to the surface, creating fractures and changing the hydraulic properties of overlying units by several orders of magnitude; high permeability pathways frequently form (Booth 2002). Bed separation fissures and vertical fissures appear in the strata above the mining face, forming a wedge-shaped fissured zone (Xu et al. 2012). Zhang and Shen (2004) summarized the issues and presented a case study for mining under water-bearing alluvium.

The Shennan mining area in northern Shanxi Province is an important coal production centre. Water resources in the area are largely limited to areas of burnt rock, unconfined aquifers, surface runoff, and reservoirs. The burnt rock lies over or under part of the coal seam that self-ignited, creating void space that has subsequently filled with water from atmospheric precipitation. This study addressed the potential future impact of large-scale mining on the area's local shallow water resources.

Research Region

The coal seams of the early Jurassic Yan'an Formation are being mined in the Ningtiaota, Zhangjiamao, and Hongliulin collieries (Table 1) in China's northern Shaanxi province, which contains 5.5 billion metric tons (t) of coal in a 373.4 km^2 area. The study sites are located in the mountain ridge and aeolian sand area (Fig. 1). Groundwater there is mainly derived from alluvial sand layers and aeolian sand dunes in the Upper Pleistocene Salawusu formation.

Drilling unit water inflow (q) is an accepted index in China for evaluating the water yield of an aquifer. The method for obtaining q is an aquifer pump test, with a pumping aperture of 91 mm. The index of q is $Q_{10}/10$, which is based on the pumping water yield when the drawdown during drilling is 10 m. A weak water yield is $q \leq 0.1$ L (s·m), a moderate water yield is 0.1 L (s·m) $< q \leq 1.0$ L (s·m), a strong weak water yield is 1.0 L (s·m) $< q \leq 5.0$ L (s·m), and very strong water yield is $q > 5.0$ L (s·m). The drilling unit water inflow of both units is weak or moderate (the burnt rock area is rich in water), except for where water flows on the surface. The Changjiagou reservoir holds 2.25 million m^3, on average.

Surface Drainage and Groundwater

The watercourse in the Kaokaowusu gully is 10–20 m wide and the flow ranges from 225 to 1404 L/s. The watercourse in the Changjia gully is 2–10 m wide and the flow is 3–635 L/s. The catchment area of the Changjiagou reservoir is 44 km^2, and its capacity is 12 million m^3. The flow in the Lucao gully is about 144 L/s and the discharge of the Majiata River is about 500 L/s. The Miao gully is 8.6 km long and its river flow is about 35 L/s. The Kentieling River (58–97 L/s) is a 3 km long branch of the Kaokaowusu gully. The Xiaohjmh gully, another 3 km branch of the Kaokaowusu gully, has a flow of 87–240 L/s. All of the gullies are shown in Fig. 1.

Table 1 shows the aquifers and aquicludes in the Shennan mining area: the Holocene alluvial and diluvial pore phreatic aquifer (Q_4^{al+pl}), the upper Pleistocene pore phreatic aquifer of the Salawusu Formation (Q_3^s), the middle Jurassic aquifer of the Yan'an Formation (J_2^y), the upper-middle Pleistocene Lishi loess (Q_2^l), and the Pliocene Baode red clay (N_2^b).

About 30 m of burnt rock (Fig. 1) overlie the 1^{-2} and 2^{-2} coal seams over an area of 300–800 m in the Ningtiaota colliery. Similar burnt rock strata (15–30 m thick) overlie the 4^{-2} and 5^{-2} coal seams in the Hongliulin and Zhangjiamao collieries.

Engineering Geology

The rock and soil mass overlying the first seam (coal 2^{-2}) in the area consists mainly of sand, soil, and bedrock (Table 2). The sand layers are rich in water and are mainly distributed in southwest Ningtiaota, Hongliulin, and west Zhangjiamao (Fig. 1). The soil layers in the north and southwest Ningtiaota, Hongliulin and northeast Zhangjiamao areas range in thickness from 20 to 70 m (Fig. 2). The bedrock layer is shown in Fig. 2.

Only the soil layers and the bedrock are observed in the mountain ridge area (Table 2). The soil layers (Q_2^l and N_2^b) have very low permeability, which restricts infiltration of atmospheric precipitation. However, due to the dense distribution of dry gullies in the area, precipitation typically drains away quickly. This surface water is used downstream for

Table 1 Stratigraphy of the study area

Strata			Lithology	Thickness/m	Geological rock group
System	Series	Formation			
Quaternary	Holocene	(Q_4^{eol})(Q_4^{al})	Aeolian sand	0–60	Sand layer group
	Upper Pleistocene	Malan (Q_3^m)	Silty sand (distributed sporadically)	0–30	
		Salawusu (Q_3^s)	Silty fine sand, clay	0–160	
		Lishi (Q_2^l)	Loam, sand paper clay	20–165	Soil layer group
Neogene	Pliocene	Baode (N_2^b)	Sand paper clay, clay	0–110	
Jurassic	Middle Jurassic	Zhiluo (J_2^z)	Mudstone, sandy mudstone, sandstone	70–134	Bedrock layer group
	Middle Jurassic	Yan'an (J_2^y)	Sandstone, mudstone, coal seams (1^{-2}, 2^{-2}, 2^{-2b}, 3^{-1}, 5^{-2})	150–280	

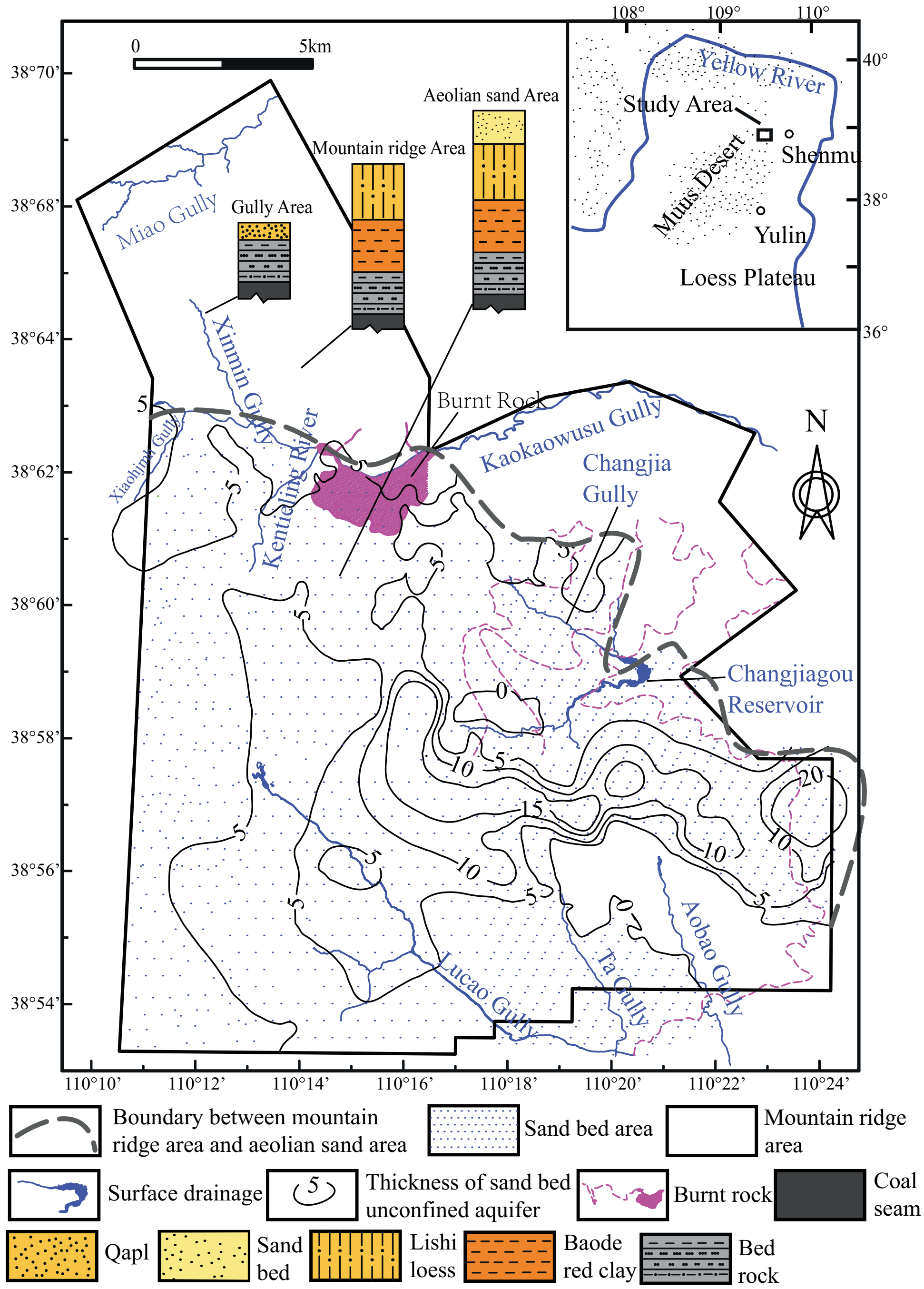

Fig. 1 Geological map of the Shennan mining area

drinking water, to irrigate 20 km^2 of farmland, and by animals. The burnt rock is considered to be a stable water resource, so if these areas are mined, lateral sublevel coal pillars should be left to prevent significant subsidence to protect them.

Method

The fractured overburden strata can be divided into four zones (Peng 1992). Water can permeate through the caved and fractured zones, which together form a "water-conducting fractured zone" (WCF; Zhang and Shen 2004). To better control surface subsidence and to safely extract coal from beneath the aquifer, the height of the mining-induced fractured zone in the overburden strata must be determined.

The Key Strata

The properties and structure of the rocks greatly affect overburden strata movement. For instance, hard and brittle strata are very susceptible to cracking and fracturing (Miao et al. 2011). Researchers in China have demonstrated that thick and hard rock layers, termed “key strata”, play an important role in controlling overburden movement (Miao and Qian 2000; Miao et al. 2005a, b; Qian et al. 1996). Supposing that there are n layers of rock strata above the coal seam, the thickness and the density of each layer are assumed to be h_i and γ_i (i = 1, 2, 3…n), respectively. If the overburden from the first layer to the nth layer are controlled by the first rock stratum, and deformation is synchronized, the overburden strata can be regarded as a composite beam. According to this concept and the deformation characteristics of the key strata, the movement and breakage of the overburden rock are synchronized to the movement and breakage of the key stratum (Miao et al. 2011). The tensile strength of the key stratum and the strain resistance of the soft rock strata can be computed for the limited span (the distance that the overburden strata fractures over the goaf), so the height of the WCF zone can be judged by the limited span of the key stratum and rock strata as well as the height of the free space below.

Rock layers are key strata when four conditions are satisfied:

1. When the unsupported part of a key stratum is less than its limited span, the WCF zone will not develop upward.
2. When the unsupported part of a key stratum is greater than its limited span, and there is no free space between two adjacent strata that have different deflections, then the WCF zone will end. Otherwise, it will continue to develop upward.
3. When the horizontal tensile strain of the soft rock is less than its horizontal limited tensile strain, the WCF zone will not develop upward.
4. When the horizontal tensile strain of the soft rock is greater than its limiting horizontal tensile strain, and the maximum deflection of the rock is greater than the free-space height below, the WCF zone ends. Otherwise, the WCF zone will keep developing upwards.

Consider an example: longwall panel 1201 is 3021 m long and 295 m wide, and was excavated by a two-entry gate road system within the no. 2^{-2} coal seam, which is 4.0 m thick. The height of the WCF zone, based on the key stratum theory, is shown in Table 2. The WCF zone will develop to or over the top of the weathering bedrock once it breaks through the No. 11 rock stratum, namely, the key stratum. At this time, the zone will be 49.36 m high. Nearly 12 m of mudstone overlies the key stratum (Table 2). Thus, even if the key stratum is broken, the mudstone will limit water transmission.

Water Conducting Height

Based on field data from more than 200 boreholes in 27 mines, Liu (1981) developed an empirical formula for predicting the height of fractured zones for different rock types, i.e., strong, medium strong, soft, and weathered soft rock.

$$H_f = \frac{100\,M}{aM + b} \pm \sigma \tag{1}$$

where H_f is the maximum height of the WCF zone evaluated from the immediate roof of the seam, in metres; M is the thickness of the extracted seam, in metres; a and b are

Table 2 Results of Key Stratum theory

	Lithology	Thickness (m)	Unit weight (KN/m^2)	Uniaxial compressive strength (MPa)	Strength of extension (MPa)	Elasticity modulus (GPa)	Bulking coefficient	Status
0	Coal 2^{-2}	4.00						
1	Mudstone	1.00	23.0	27.1	1.20	3.10	1.02	Caving
2	Siltstone	2.13	25.0	32.3	4.60	14.0	1.03	Caving
3	Fine ss.	7.20	24.1	42.1	4.30	15.0	1.03	Hard stratum
4	Siltstone	11.61	24.5	35.4	4.7	14.5	1.03	Hard stratum
5	Med. ss.	7.5	24.2	45.3	3.3	17	1.03	Soft stratum
6	Fine ss.	9.70	24.3	43.5	4.20	16.7	1.03	Hard stratum
7	Mudstone	0.60	23.1	28.0	1.30	3.40	1.02	Soft stratum
8	Coal 1^{-2}	1.48	13.2	15.0	1.20	2.40	1.05	Soft stratum
9	Silty ms.	3.74	23.2	40.2	1.4	3.9	1.025	Soft stratum
10	Siltstone	4.90	25.2	34.9	4.5	13.6	1.03	Hard stratum
11	Fine ss.	16.1	24.3	43.0	4.40	17.7	1.03	Main key stratum

ss. sandstone, *ms.* mudstone

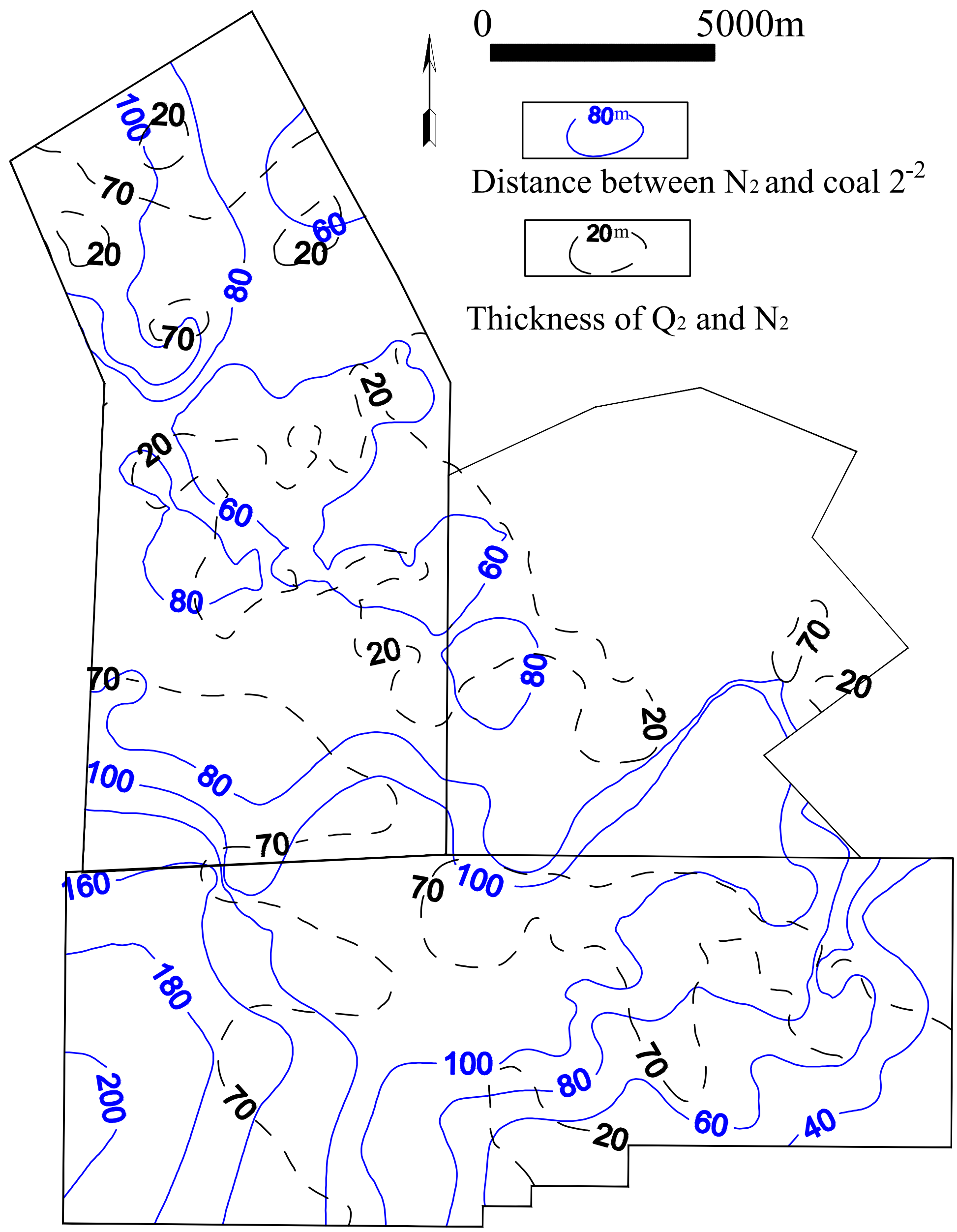

Fig. 2 Thickness chart of the soil and rock layer group

coefficients that are based on the strata lithology, and σ is the mean square deviation, in metres (Table 3).

In China, a national standard also offers empirical formulas (Table 4). However, formula (1), Tables 3 and 4 are only suitable for predicting the height of fractured water-conducting zones for a single slice extraction with a height of 1–3 m and a cumulative total mining height <15 m.

Fifteen measured values and seven key stratum calculated values for the Hongliulin coal mining area were used for fitting the height of the WCF zones (Table 5; Fig. 3). The linear fitting results can be obtained using formula (2).

$$H_f = 9.59M + 13.55 \tag{2}$$

where H_f is the maximum height of the WCF zone in metres; and M is the thickness of the extracted seam in metres.

When the mining height was 1 to 3 m, the WCF zone heights calculated using the three formulae were very close (Fig. 3), indicating that the empirical results obtained by the fitting formula align with other mining areas. With greater mining heights (3–6 m), the height of the WCF zone generally increased (Fig. 4), but the increment calculated using the ES formula was greater than that calculated using the

Liu and fitting formulae for the same mine height increment. When the mining height exceeded 6 m, the fitting formula result was larger than that obtained using the ES and Liu formulae. The increment in the fitting formula is equal to that of the ES formula for the same mining height increment, so the fitting formula is more suitable for forecasting the height of the WCF zone in this area.

Pumping Tests

Coal mining causes stress redistribution, which causes compression and shearing of clay layers, leading to a change in the clay structure as well as a huge change in its permeability. Pressure water tests were carried out on site to accurately ascertain how clay permeability changed before and after mining.

Before the S1501 working face of the Hongliulin mining area was developed, a well (HL2) was constructed 50 m from the first cutting roadway, and a pumping test was carried out in well HL2. Water was injected into the loess and red clay at an initial pressure of 1.0 MPa. Then, the injection was repeated at 0.6 Mpa, and then at 0.3 MPa.

Table 5 Values of height of water-conducting fractured zones

Measured values						Calculated values	
Mining thickness	WCFZ	Mining thickness	WCFZ	Mining thickness	WCFZ	Mining thickness	WCFZ
2.0	33	4.5	60	4.0	46	1.6	28
2.5	38	5.0	65	4.0	57	2.0	32
3.0	46	5.5	71	4.0	45	4.0	44
3.5	52	5.5	67	4.0	45	4.0	45
3.6	69	6.0	77	5.0	41	4.0	50
4.0	57	11.9	129				

Table 3 Parameters for predicting the height of the water-conducting fractured zone (Liu 1981)

Rock type	UCS/MPa	Representative rock	Formula
Hard and strong	>40	Quartz sandstone, limestone	$H_f = \frac{100\sum M}{1.2\sum M + 2.0} \pm 8.9$
Medium hard	20–40	Sandstone, sandy shale	$H_f = \frac{100\sum M}{1.6\sum M + 3.6} \pm 5.6$
Soft and weak	10–20	Mudstone, argillaceous sandstone	$H_f = \frac{100\sum M}{3.1\sum M + 5.0} \pm 4.0$
Weathered soft and weak	<10	Bauxitic roc, weathered mudstone, clay	$H_f = \frac{100\sum M}{5.0\sum M + 8.0} \pm 3.0$

M-accumulated mining thickness, m

Table 4 Empirical formulae of maximum height of the water-conducting fractured zone (ES)

Coal bed pitch/°	USC/MPa	Rock type	Roof management	Height of water-conducting fractured zone/m
0–54	40–60	Diabase, limestone, siliceous quartzite, conglomerate, glutenite	All fall	$H_f = \frac{100M}{2.4n + 2.1} + 11.2$
	20–40	Arenaceous shale, argillaceous shale, shale	All fall	$H_f = \frac{100M}{3.3n + 3.8} + 5.1$
	<20	Decayed rock, shale, argillaceous sandstone, clay rock	All fall	$H_f = \frac{100M}{5.1n + 5.2} + 5.1$
55–85	40–60	Diabase, limestone, siliceous quartzite, conglomerate, glutenite	All fall	$H_f = \frac{100mh}{4.1n + 133} + 8.4$
	<40	Decayed rock, shale, argillaceous sandstone, clay rock	All fall	$H_f = \frac{100mh}{7.5n + 293} + 7.3$

M-accumulated mining thickness, m; n- number of layers of slicing mining; m-coal thickness, m; h- vertical height of panel, m

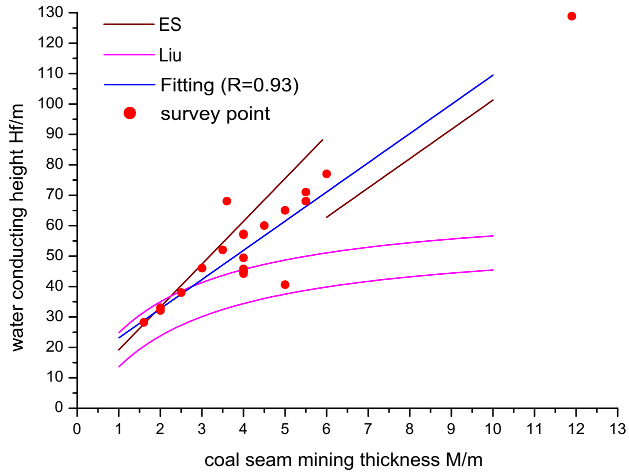

Fig. 3 Comparison of Liu's empirical formula (Eq. 1), ES empirical formula (Table 4) and Fitting formula (Eq. 2)

When the working face (S1501) had moved 100 m, well HL3 was constructed 50 m from the same roadway and the successive injections into the loess and red clay were repeated. The water flow was observed under the different pressures and the permeability coefficients (Fig. 5) were calculated using Formula (3).

$$k = \frac{Q}{2\pi Hl} \ln \frac{l}{r_0} \quad (3)$$

where K is the permeability coefficient, in m/d; Q is the water yield, in m^3/d; H is the water head, in m; l is the pumping test length, in m; and r_0 is the radius of the well, in m.

The loess and the red clay in well HL2 were 42.8 and 41.4 m thick, respectively (Fig. 4). The height of the WCF zone at HL3 did not enter into the red clay layer but reached the bottom of the weathered rock stratum. Before mining, the permeability coefficient of the loess was greater than that of the red clay. After mining, the permeability coefficient of the loess changed substantially while that of the red clay changed very little, thus confirming the impermeability of the red clay.

Results

The shallow water resources in the Shennan mining area mainly consist of phreatic water in a sand layer. The aquifuge is the Baode red clay. When the highest point of the WCF zone was below the Baode clay, the low permeability of the loess and red clay protected the shallow water from leakage. Where the WCF zone penetrated the loess, the shallow water leaked completely. When the highest point of the WCF zone was in the aquifuge, the red clay was partially cracked, making it important to establish how thick the red clay stratum had to be to protect the surface water.

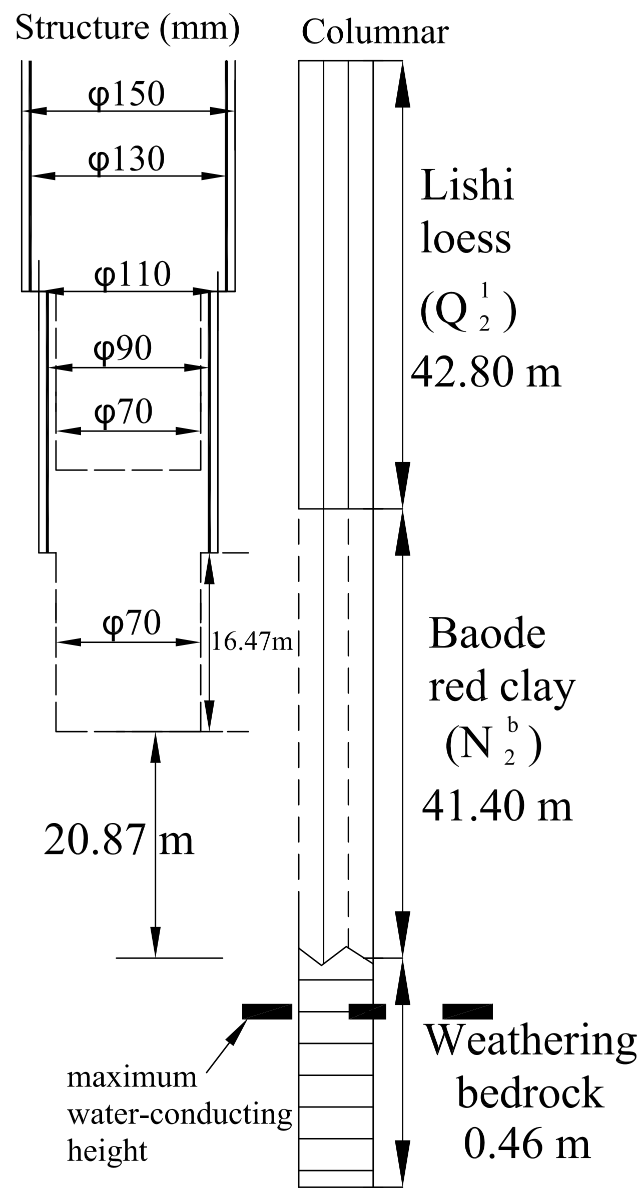

Fig. 4 Permeability coefficient of Lishi loess (Q2) and Baode red clay (N2)

Water Equilibrium Theory

The impact of large-scale total-extraction mining on groundwater resources needs to be considered in mine design. When the leakage of underground phreatic water through the clay layer is more than the exploitable amount of groundwater, water loss is serious. The exploitable amount of water in

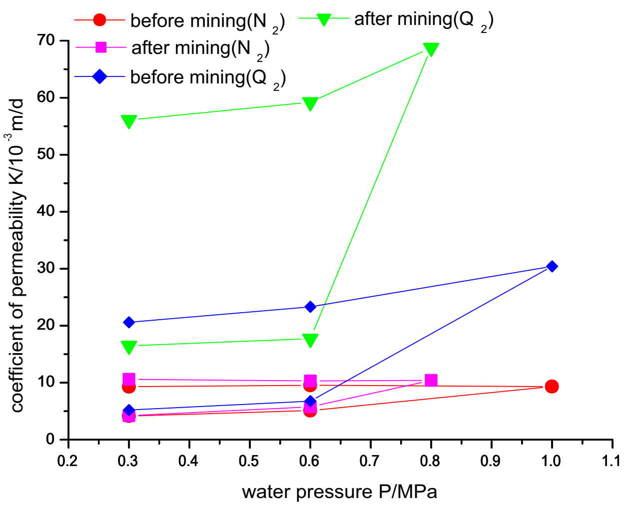

Fig. 5 Stratigraphy and structure of pumping test in drill hole

Table 6 Pumping test data

Drill hole	Average water output (m^3/d)	Water level fall (m/d)
N355	736.991	5.80
KT33	695.263	5.45

the sand layer area can be calculated according to the water equilibrium method:

$$W' = \Delta W_b + \Delta W_p \quad (4)$$

where W' is leakage, in m^3; ΔW_b is groundwater recharge, in m^3; ΔW_p is the reduced natural output induced by phreatic water leakage, in m. In the Shennan mining area $\Delta W_b \approx 0$, and $W' = \Delta W_p$.

After investigating the area, we determined that the difference between the flow-in and flow-out water in Kaokaowusu gully was 201 L/s, the amounts of water flowing in the Changjia and Lucao gullies were 178 L/s and 142 L/s, respectively, and the other discharge was 891 L/s, for a total of 1412 L/s (122,000 m^3/d). The exploitable amount can also be determined by a pumping test (Formula 5).

$$Q_c = Q_b + \mu F \Delta v \quad (5)$$

where Q_c is the pumping water yield, in m^3/d; Q_b is the supplementary amount, in m^3/d; μF is the unit of storage capacity, in m^3/m; and Δv is the average water level drop speed, in m/d. The pumping test data are shown in Table 6. The values of Q_b (45.46 m^3/d) and μF (119 m^2) are obtained from the data in Table 6 and Formula (5).

The height of the WCF zone is predicted to develop to the water-resisting soil layer in the study area, so a portion of the water resource will leak through this soil layer. Groundwater leakage in this area was calculated using Formula (6).

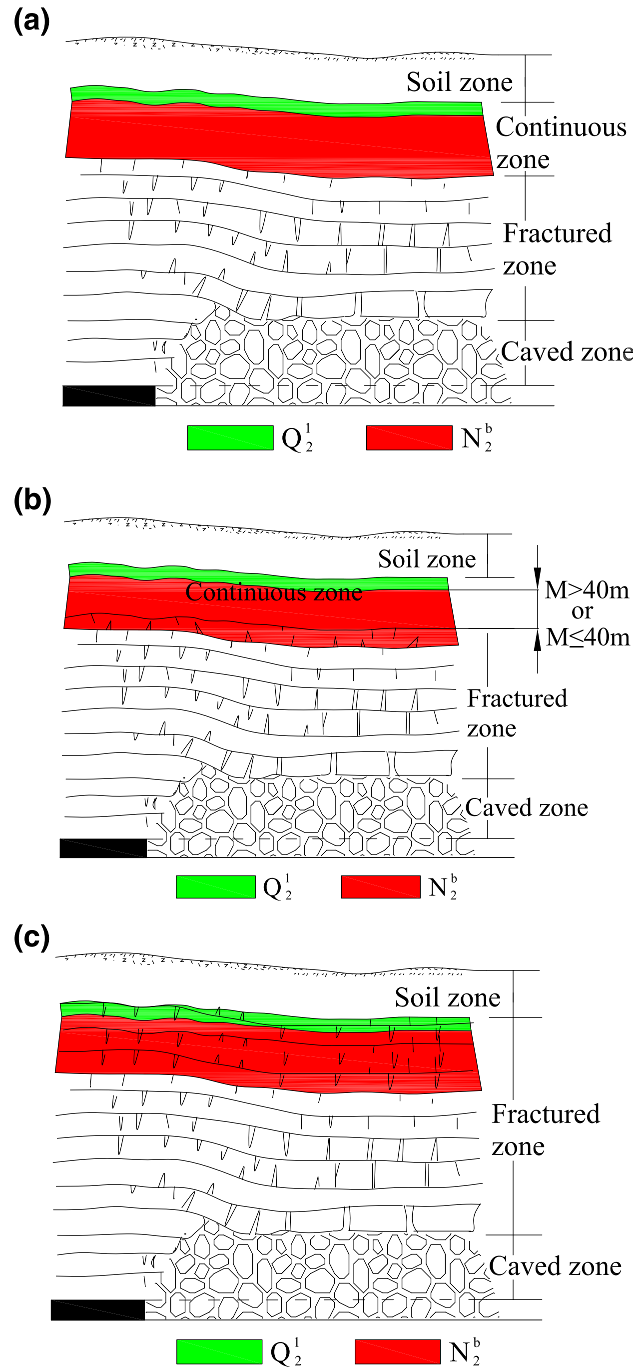

Fig. 6 Degree of water loss (**a** no water loss; **b** slight or moderate water loss; **c** serious water loss)

$$W' = K_e \Delta H F t \quad (6)$$

where W' is groundwater leakage, in m^3; $K_e = K'/M'$, K is the permeability coefficient of the clay layer, in m/d, and M' is the unbroken thickness of the clay layer, in m; ΔH is the height of the water head of phreatic water, in m; F is the osmosis area, in m^2; and t is the osmosis time, in d.

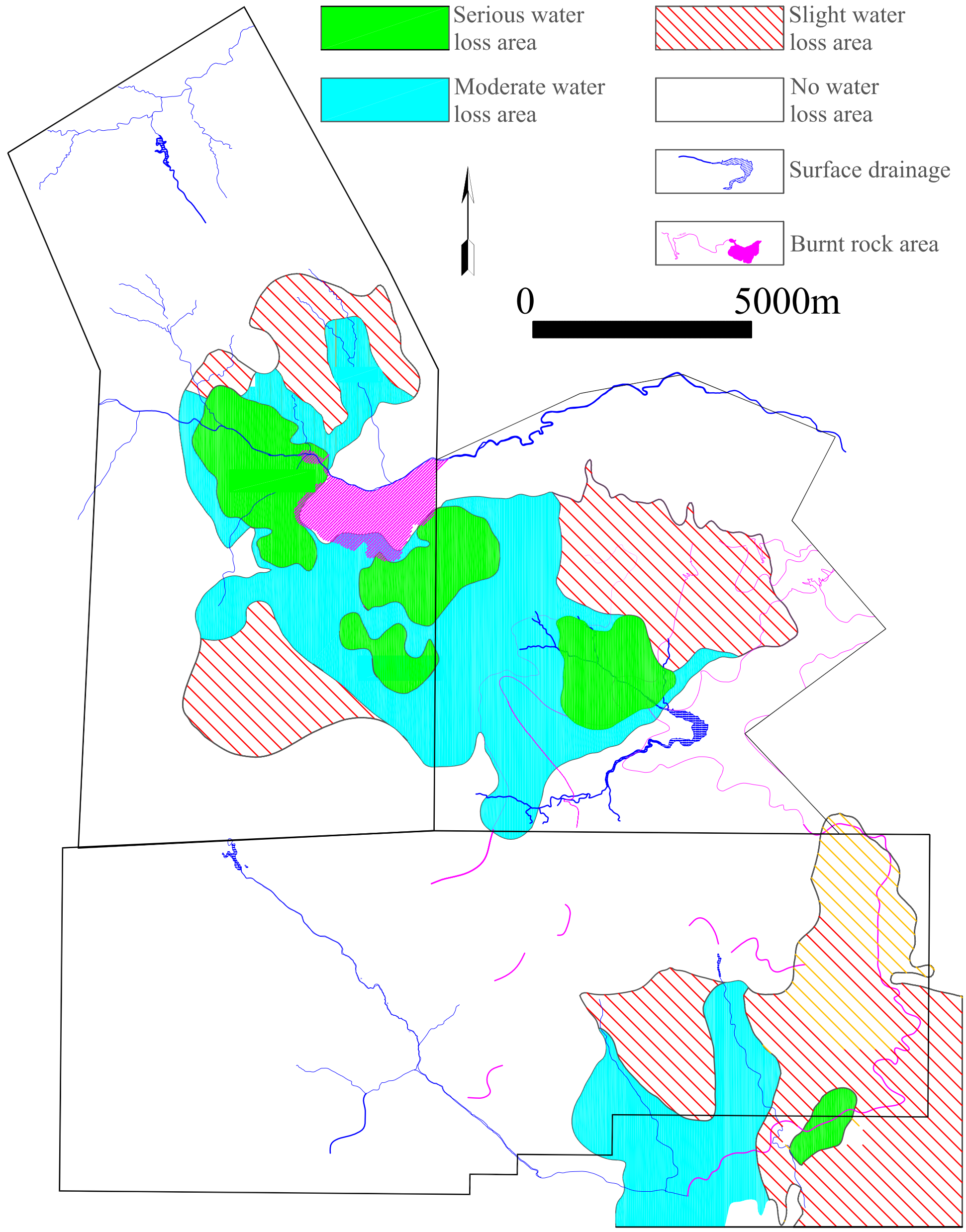

Fig. 7 Sketch map showing the extent of shallow water loss induced by coal mining

When the parameters obtained by the water equilibrium method were substituted into Formula (6), ΔH was the distance from the natural discharge datum level to the bottom of the average sand layer (5 m) and K' was the average permeability coefficient (0.06876 m/d). The area of this region (F) is 14,420,000 m^2; therefore, $M' = 40.62$ m.

When the parameters obtained by the pumping test method were substituted into Formula (6), ΔH was the distance from the natural discharge datum level to the bottom of the average sand layer (5 m) and K' was the average permeability coefficient (0.06876 m/d). The area of this region (F) is 5950 m^2, and the supplementary amount (Q_b) while pumping is 45.46 m^3/d, thus $M' = 45.00$ m.

Based on these two methods, when the residual thickness of Baode red clay is >40 m, leakage of water resources will be slight. When the residual thickness is <40 m, leakage will be moderate.

Engineering Geological Zonation

The leakage of the shallow sand layer aquifer can be classified based on the height of the WCF zone and the thickness of the Baode red clay layer. When the highest point of the WCF zone is below the Baode clay layer and the thickness of the clay exceeds 40 m, the shallow sand layer aquifer will not leak ("no water loss"). When the WCF zone develops into the Baode red clay layer and the thickness of the uncracked clay layer exceeds 40 m, the leakage can be defined as "slight". When the WCF zone enters into the clay layer and the thickness of the uncracked red clay is <40 m, the leakage type can be defined as "moderate". When the WCF zone passes through the Baode clay layer, the leakage can be defined as "serious". These four water loss types are illustrated in Figs. 6 and 7.

Conclusion

The overburden in the study area can be divided into a sand, soil, and bedrock. The sand layer is not found in the mountain ridge area, and therefore shallow water resource leakage is not a concern there. Surface water and burnt rock strata were the water resources most seriously affected by mining, and for this reason, coal seams beneath these areas are not allowed to be mined. Since the aeolian sand, part of the soil layer group, can have variable thicknesses, mining beneath it should also be controlled. The empirical formulae (ES and Liu) developed for predicting the height of the WCF zone are applicable for coal seams <3 m thick, but the coal seam in the study area is 4 m thick. The height of the WCF zone calculated by the key stratum theory was close to the measured value, so a comprehensive fitting analysis was conducted to develop a WCF zone calculation formula for the study area. Pumping tests showed that the red clay was the effective water-resisting layer and so, based on the water equilibrium theory, it was determined that a residual thickness of at least 40 m of the red clay can resist water effectively.

The influence of coal mining in the aeolian sand area on the shallow water resources was divided into four categories: serious, moderate, slight, and no water loss. This research should be of significant value in protecting the area's local shallow water resources, though additional work is still needed.

Acknowledgments Financial support for this work was provided by the State 973 Project (Grant 2015CB251601), the Fundamental Research Funds of the State Key Program of National Natural Science of China (Grant 41430643), the Fundamental Research Funds for the Central Universities (2015QNB23), and the Priority Academic Program Development of Jiangsu Higher Education Institutions. The authors also thank the anonymous reviewers for their helpful comments.

References

Adam PJ, Paul LY (2000) Broadening the scope of mine water environmental impact assessment: a UK perspective. Environ Impact Asses 20:85–96

Andreas K, Nikola R (2011) Special issue: sustainable development of energy, water and environment systems. Water Resour Manage 10:33–39

Booth CJ (2002) The effects of longwall coal mining on overlying aquifers. Geol Soc Spec Publ 198:17–45

Chi JG, Wang XE, Qi EQ, Luo XL (1991) Exploration Specification of Hydrogeology and Engineering Geology in Mining Areas. General Administration of Quality Supervision, Inspection and Quarantine of the People's Republic of China (AQSIQ), GB 12719-91, Beijing

Hickcox DH (1980) Water rights, allocation and conflicts in the Tongue River Basin, Southeastern Montana. J Am Water Resour Assoc 16(5):797–803

Karen LJ, Paul LY (2006) The co-treatment of sewage and mine waters in aerobic wetlands. Eng Geol 85:53–61

Kendorski FS (1993) Effect of high-extraction coal mining on surface and ground waters. In: Peng SS (ed) Proc, 12th International Conf on Ground Control in Mining, Morgantown, WV, USA, pp 228–235

Liu T (1981) Coal mine ground movement and strata failure. Coal Industry Publication House, Beijing

Liu TQ (1981) Surface movements, overburden failure and its application. Coal Industry Press, Beijing (**in Chinese**)

Miao XX, Qian MG (2000) Advance in key strata theory of mining rockmass. J Min Technol 29(1):25–29 (**in Chinese**)

Miao XX, Mao XB, Sun ZW, Pu H (2005a) Formation conditions of compound key strata in mining overlayer strata and its distinguishing method. J Chin U Min Technol 34(5):547–550 (**in Chinese**)

Miao XX, Chen RH, Pu H, Qian MG (2005b) Analysis of breakage and collapse of thick key strata around coal face. Chin J Rock Mech Eng 24(8):1290–1295 (**in Chinese**)

Miao XX, Cui XM, Wang JA (2011) The height of fractured water-conducting zone in under mined rock strata. Eng Geol 120:32–39

Peng SS (1992) Surface Subsidence Engineering. SME, New York City

Peng SS (2008) Coal Mine Ground Control (3rd Edit). Science Press, Beijing

Qian MG, Miao XX, Xu JL (1996) Theoretical study of key stratum in ground control. J Chin Coal Soc 21(3):225–230 (**in Chinese**)

Qiao W, Li W, Zhang X (2014) Characteristic of water chemistry and hydrodynamics of deep karst and its influence on deep coal mining. Arab J Geosci 7:1261–1275

Singh R, Atkins A (1982) Design considerations for mine workings under accumulations of water. Int J Mine Water 1:35–56

Sun W, Wu Q, Dong DL, Jiao J (2012) Avoiding coal-water conflicts during the development of China's large coal-producing regions. Mine Water Environ 31:74–78

Tan JW (2008) Mine Environment Technology. Di Zhen Publ House, Beijing (**in Chinese**)

Thomas JL, Anderson RL (1976) Water-energy conflicts in Montana's Yellowstone River Basin. J Am Water Resour As 12(4):829–842

Tieman GE, Rauch HW (1987) Study of dewatering effects at an underground longwall mine site in the Pittsburgh seam of the northern Appalachian Coalfield. Proc, US Bureau of Mines Technology Transfer seminar, Pittsburgh, PA, USA, pp 72–89

Wu Q, Chen Q (2008) An analysis of environmental effects induced by environmental problems in mines. Hydrogeol Eng Geol 5:81–85

Wu Q, Li Z (2002) Prevention and Control of Mine Flood (Class A). China Univ of Mining and Technology Publ House, Xuzhou

Xu XL, Zhang N, Tian SC (2012) Mining-induced movement properties and fissure time–space evolution law in overlying strata. Int J Rock Mech Min Sci 22:817–820

Zhang JC, Shen BH (2004) Coal mining under aquifers in China: a case study. Int J Rock Mech Min Sci 41:629–639

Zhang F, Chen L, Zhang S, Zhao H, Hou X (2009) Research on feedback effect between energy development and geological environment. Geological Publ House, Beijing (**in Chinese**)